



How foam stability against drainage is affected by conditions of prior whey protein powder storage and dry-heating: A multidimensional experimental approach

Alexia Audebert, Sylvie Beaufils, Valérie Lechevalier-Datin, Cécile Le Floch-Fouéré, Arnaud Saint-Jalmes, Stephane Pezenec

► To cite this version:

Alexia Audebert, Sylvie Beaufils, Valérie Lechevalier-Datin, Cécile Le Floch-Fouéré, Arnaud Saint-Jalmes, et al.. How foam stability against drainage is affected by conditions of prior whey protein powder storage and dry-heating: A multidimensional experimental approach. Journal of Food Engineering, 2019, 242, pp.153-162. 10.1016/j.jfoodeng.2018.08.029 . hal-01868078

HAL Id: hal-01868078

<https://hal.science/hal-01868078>

Submitted on 28 Sep 2018

HAL is a multi-disciplinary open access archive for the deposit and dissemination of scientific research documents, whether they are published or not. The documents may come from teaching and research institutions in France or abroad, or from public or private research centers.

L'archive ouverte pluridisciplinaire **HAL**, est destinée au dépôt et à la diffusion de documents scientifiques de niveau recherche, publiés ou non, émanant des établissements d'enseignement et de recherche français ou étrangers, des laboratoires publics ou privés.



Distributed under a Creative Commons Attribution - NonCommercial - NoDerivatives 4.0 International License

How foam stability against drainage is affected by conditions of prior whey protein powder storage and dry-heating: a multidimensional experimental approach

(Alexia Audebert)^a, Sylvie Beaufils^b, Valérie Lechevalier^a, Cécile Le Floch-Fouéré^a, Arnaud Saint-Jalmes^b, Stéphane Pezennec^a

^a STLO, UMR1253, INRA, Agrocampus Ouest, F-35000, Rennes, France

^b Institute of Physics Rennes, UMR6251 UR1-CNRS, Rennes University, F-35000, Rennes, France

stephane.pezennec@inra.fr

Abstract

In the present work, we investigated the effects of powder dry-heating parameters on whey protein foams stability, especially against drainage.

To this aim, whey protein isolate solutions were prepared at various pH (3.5, 5.0, 6.5), with or without a prior dialysis step to reduce the lactose content, freeze-dried, adjusted to various levels (0.12, 0.23, 0.52) of powder water activity a_w and dry-heated at 70 °C for up to 125 h. Protein solutions were then reconstituted at pH 7.0 and foams prepared by air bubbling.

An original approach was followed to study the foam stability against drainage, involving monitoring of the liquid fraction as a function of both height in the foam column and time, and analysing the whole set of time and height liquid fraction profiles using multivariate statistics.

The effects of dry-heating parameters were markedly interdependent, resulting in complex effects on foam stability. However, the results suggest that dry-heating at pH 3.5 increased foam stability. Moreover, the a_w adjustment step, though consisting in a two-week pre-conditioning at room temperature, also had a significant effect on the foam stability, of the same order of magnitude as dry-heating effects.

Keywords

Dry-heating; Whey protein powder; Foam stability; Water activity; pH; Lactose

1. Introduction

Liquid foams are concentrated dispersions of gas bubbles in a liquid continuous phase. They are thermodynamically unstable, due to destabilisation processes such as liquid drainage, disproportionation and coalescence. Foam drainage is the flow of liquid under the influence of gravity. It leads to foam drying, which promotes the rupture of thin liquid films separating adjacent bubbles, namely coalescence events. Disproportionation is the surface-tension-driven gas exchange from small to large bubbles due to the difference in internal pressure (Laplace's law), favouring the growth of the average bubble size with time. Their limitation is crucial to obtain a better foam stability (Cantat et al., 2013).

Due to their amphiphilic nature, proteins adsorb to hydrophobic interfaces. At the air-water interface and in aqueous foams, they can reduce surface tension and form a visco-elastic interfacial film surrounding the gas bubbles, thus helping the formation and stabilisation of foams. Protein foam formation depends on their surface activity and their adsorption kinetics, while foam stability depends on the film mechanical properties (Narsimhan and Xiang, 2017). Protein foam structure can be described at different length scales. First, an adsorbed protein layer ($\approx 10^{-10}$ - 10^{-8} m) separates the solution from air. Second, neighbouring bubbles are separated by a liquid film, or lamellae ($\approx 10^{-8}$ - 10^{-6} m), with two air-water interfaces. Third, three films junction forms a canal called Plateau border ($\approx 10^{-6}$ - 10^{-4} m) (Cantat et al., 2013).

In food sciences, measurements of protein foam stability generally integrate the consequences of all the instability mechanisms in a global stability, such as the time at which the first drop drains or the cumulative weight of drained liquid as a function of time (Nicorescu et al., 2011). In the present study, we developed an original methodology to characterise in more details the protein foam stability against drainage, by transposition of a foam physics approach. More precisely, we analysed whole time and height profiles of liquid fraction in foams, in conditions where drainage is the prominent destabilisation mechanism. Multivariate statistics were used to extract essential information from the whole data set.

After cheese and casein manufacturing, a fluid called whey remains, mainly composed of water, lactose (4.8 %) and protein (0.7 %). Whey is processed by separation technologies and dried into food ingredients such as whey protein isolates (WPI) (>90 % of protein). In WPI, the main proteins are β -lactoglobulin (β -lg) and α -lactalbumin (α -la) (Ortega-Requena and Rebouillat, 2015). Whey proteins have attracted considerable interest because of their high nutritive value and functional properties. Their use in food formulation is based on their aptitude to increase viscosity, gelling, water binding, emulsion or foam stability (Ortega-Requena and Rebouillat, 2015). They are found in a large diversity of aerated food products like aerated desserts, whipped cream, and cappuccino foam (Narsimhan and Xiang, 2017).

Whey protein heating is a commonly used processing operation for changing techno-functionalities. Heating denatures proteins which enhances the exposition of buried hydrophobic amino acid residues. Then, aggregation of proteins can occur by covalent bonding and hydrophobic interactions (Anema, 2014). The coexistence of non-aggregated and aggregated proteins is important for foaming properties. Non-aggregated proteins contribute to the foam formation because they adsorb quickly at the interface. Aggregated proteins, depending on the structure and the size, can modify the bulk rheology and slow down the drainage by their presence in the Plateau borders (Fameau and Salonen, 2014). In the case of in-solution heating of WPI, Schmitt et al. (2014); Lazidis et al. (2016) have

demonstrated that specific aggregates, called microgels, greatly increase foams stability through a reduced drainage, by increasing the bulk viscosity. Aggregates may also contribute to interfacial layer properties (Fameau and Salonen, 2014). Indeed, interfacial rheology is a key factor in foam stability (Narsimhan and Xiang, 2017).

Dry-heating of egg white powder is commonly applied to maintain the microbiological quality and improve foaming and gelling properties (Boreddy et al., 2016). In comparison with heating of liquid solutions, dry-heating of protein powders is a way to disconnect proteins denaturation and aggregation and also to obtain different protein structural modifications (Desfougères et al., 2011; Gulzar et al., 2011; Povey et al., 2009). Indeed, Desfougères et al. (2011) showed that slight structural modifications of lysozyme are sufficient to greatly improve interfacial properties and foam stability. Usually, molecular motion is reduced in powders because of their amorphous glassy state at room temperature. Consequently, reaction kinetics are considerably slowed. The powder water activity (a_w) is a crucial parameter. As an example, the denaturation temperature of proteins in a WPI powder is 175°C, 163°C and 132°C at different a_w 0.11, 0.23, 0.53 respectively (Zhou and Labuza, 2007). Dry-heating time and pH prior to dehydration also affect both the type and kinetics of reactions in a WPI powder, and its gelling (Gulzar et al., 2011, 2012). The lactose content in WPI also plays a key role in functional properties (Guyomarc'h et al., 2015). The Maillard reaction occurs in dairy products subjected to heat treatment, drying or storage. The first step is the lactosylation: lactose condenses with a protein amino groups to form a Schiff base. In a later stage, a complex form of non-enzymatic browning is produced (Arena et al., 2017).

Dry-heating could be a way to improve the techno-functionality of WPI. However, only a few investigations on the foaming properties of dry-heated whey proteins have been reported. Some report that the effect of dry-heating on the foaming properties of WPI powder strongly depends on the dry-heating conditions (time, temperature, a_w) (Radwan et al., 1993; Norwood et al., 2016). The effect of dry-heating of β -lg powder with sugars on foam stability depends also on the sugar nature (Medrano et al., 2009; Corzo-Martínez et al., 2012). Thus, in this study, we examined the effect of parameters like time, a_w , pH prior to dehydration and lactose content on the WPI foaming properties. Our multifactorial experimental design allowed us to highlight the complex interactions between parameters.

The originality of our experimental approach consist of i) the multifactorial experimental design, ii) the bi-dimensional monitoring of foam stability as a function of both time and height and iii) the multivariate statistical analysis of the data set.

2. Materials and Methods

2.1 Powder characterisation

A unique batch of whey protein isolate (WPI) powder was used for all the experiments. It was obtained by spray-drying a whey protein concentrate isolated from milk microfiltrate by ultrafiltration and diafiltration, as described by (Chevallier et al., 2018). The nitrogen content (TN), non-protein nitrogen (NPN) and non-casein nitrogen (NCN) of the powder were determined by the Kjeldahl method (Schuck et al., 2012). The protein content was calculated by $(TN - NPN) \times 6.38$ (eq. 1). The amount of casein or insoluble proteins at pH 4.6 was measured by $(TN - NPN - NCN) \times 6.38$ (eq. 2). Free lactose in the WPI powder was measured by ion-exchange high performance liquid

111 chromatography (HPLC, Dionex, Germering, Germany) using an Aminex A-6 column (Biorad, St
112 Louis Mo., USA) and a differential refractometer (model RI 2031 plus, Jasco). The oven was kept at
113 60°C and the elution flow was 0.4 mL·min⁻¹ using a 5 mM H₂SO₄ buffer.

114 The WPI powder contained 95.0 ± 0.2 % (w/w) of proteins (calculated from eq. 1), among which
115 9.40 ± 0.04 % (w/w) of caseins or insoluble proteins at pH 4.6 (calculated from eq. 2), and
116 2.00 ± 0.02 % (w/w) of free lactose.

117 2.2 Preparation of dry heated powders

118 2.2.1 Sample preparation

119 Spray-dried WPI was dissolved in 15 mΩ resistivity osmosed water at a 7 % protein concentration. A
120 part of samples (name prefixed with “D” in the following) was dialysed against water to reach 0.2 %
121 (w/w) of lactose (10-fold reduction) (Fig. 1). The other part of samples (name prefixed with “L”) was
122 kept at their initial lactose content 2 % (w/w). Each sample was adjusted at pH 4.6 with 12 N HCl and
123 centrifuged for 30 min at 9000×g. The supernatant contained a residual amount of caseins and
124 proteins insoluble at pH 4.6 of 5.89 % (w/w) calculated from eq. 2. Then, the pH of the solution was
125 adjusted to 3.5, 5.0 or 6.5 using 12 N HCl or 12 N NaOH, and then lyophilised. Lyophilised powders
126 were adjusted to water activities of 0.12, 0.23, or 0.52 by storage for two weeks at room temperature
127 in desiccators containing saturated LiCl, MgCl₂ or Mg(NO₃)₂ solutions, respectively. Water activity of
128 commercial dairy powders is usually close to 0.23. The water activity of powders before and after
129 dry-heating was checked using an a_w-meter (Novasina, Axair Ltd, Switzerland). Powders were then
130 dry-heated at 70°C for 0, 1, 5, 25 or 125 h in hermetically sealed bottles. Control samples were
131 evaluated at intermediate stages of sample preparation (Fig. 1). Sample (1) underwent only the
132 precipitation at pH 4.6. Samples (2) and (3) were also freeze-dried at pH 3.5 and 6.5, respectively.

133 2.2.2 Experimental design

134 A multifactorial experimental design was built with pH, a_w and dry-heating time as variables. Since
135 the complete design would need 45 combinations (3 pH × 3 a_w × 5 time periods), a fractional design
136 of 20 conditions were selected by a backward selection algorithm, based on the maximisation of the
137 information matrix determinant (D-efficiency), with the Statgraphics software (Statgraphics
138 Technologies, Inc).

139 To focus on samples adjusted at pH 3.5, and to obtain a complete design in this condition, 8 trials
140 were added to the formerly described fractional design. The resulting overall design consisted of 28
141 trials. This design was used with and without lactose separately, leading to 56 conditions (including
142 30 conditions at pH 3.5). For all of them, experiments have been at least duplicated. For some of
143 them, experiments have been repeated 3 times or more. Including repetitions, 143 foams have been
144 studied.

145 2.3 Foam generation and drainage rate

146 Powders were dissolved in ultrapure water at a protein concentration of 1.9 g·L⁻¹. Each solution was
147 then dialysed against water, in order to suppress ionic strength differences between samples. During
148 dialysis, pH drifted toward the average isoelectric point of whey proteins, close to 5.0 ± 0.2. After
149 dialysis, pH was adjusted to 7.0 (NaOH 1N).

Foams were obtained by bubbling air into the protein solution (40 mL) through a porous glass disk placed at the bottom of a column until contact of the foam with the top e01 electrode (Fig. 2). The foaming time was lower than 1 min. The mean foam bubble diameter was smaller than 1 mm (Fig. 3). The conductivity of a freshly-produced foam was measured by an impedance meter operating at a frequency of 1 kHz and voltage level of 1.0 V. The liquid volume fraction φ ($\varphi = V_{\text{liquid}} / V_{\text{foam}}$) at each electrode position was measured using the empirical relationship of Feitosa et al. (2005):

$$\text{(eq 3)} \quad \varphi = \frac{3\sigma(1+11\sigma)}{1+25\sigma+10\sigma^2}$$

where σ was the relative conductivity $\sigma_{\text{foam}}/\sigma_{\text{solution}}$.

The liquid fraction φ in the foam was monitored for each electrode (at different column heights) as a function of time (Fig. 4). Liquid drained from the top to the bottom of the foam because of gravity. Thus, a gradient of liquid fraction took place along the height of the foam column and the foam was dryer at the top. In this situation, called free drainage, the evolution of the liquid fraction at a given height finally reached a power-law regime, on timescales much longer than the initial foaming time (Koehler et al., 2000; Saint-Jalmes and Langevin, 2002):

$$\text{(eq 4)} \quad \varphi \propto t^{-\alpha} \text{ where } \alpha \text{ is the free-drainage exponent.}$$

When t tends to the foaming time, there is a cut-off and φ tends to its initial value.

In other words, when drainage was the only instability phenomena occurring in the foam, the liquid fraction evolved linearly with time in log-log representation. The exponent α describes the drainage rate (Fig. 4). The lower α , the higher the foam stability against drainage. Among the electrodes pairs, only e03, e04, e05, e06 and e07 were selected for data analysis. e01, e02, e08, e09 and e10 were excluded because of boundary conditions (capillary liquid holdup at the bottom and finite size effects on the top of the foam) (Saint-Jalmes, 2006).

2.4 Statistical analysis

2.4.1 Principal Component Analysis

Principal component analysis (PCA) is a multivariate statistical method used to extract the main information from a data set, based on correlations between variables. New orthogonal variables, consisting in linear combinations of the initial variables and called principal components (PC), are computed together with the values of these new variables (scores) for each observation. Principal components are usually ordered by decreasing order of variance, in such a way that the first few principal components provide a summary of variability in the data set. Scores of observations on principal components allow to draw similarity maps where each observation is represented by a point (Abdi and Williams, 2010).

In the input of PCA, observations were foams and each foam was described by its liquid fraction measured as a function of electrode (i.e., height) and time (Fig. 4). Liquid fraction was measured every 6 seconds for 1422 s, at electrodes e03 to e07. All the data were converted into log values in order to compare the drainage exponents for different samples (Koehler et al., 2000; Saint-Jalmes and Langevin, 2002).

PCA was performed separately on the data set obtained from the fractional design (143 foams corresponding to 56 combinations of pH, a_w , heating time and lactose) and on the complete design at pH 3.5 (76 foams corresponding to 30 combinations of a_w , heating time and lactose).

2.4.2 Analysis of Variance

Analysis of variance (ANOVA) was used to test the effects of parameters (pH prior to dehydration, a_w of powders, dry-heating times and lactose content), treated as qualitative, categorical variables, on foam coordinates (scores) on the first two principal components PC1 and PC2. The normal distribution of the data and the homoscedasticity of the samples were checked. Main effects and second order interactions have been taken into account. Only effects significant at the $p < 0.01$ level have been considered and will be discussed. ANOVA was performed using the R software package (R Core Team, 2017).

3. Results

3.1 A new approach for proteins foams properties

Fig. 4a and 4b show typical log-log plots of conductivity in foams, converted to liquid volume fraction, as a function of time, for different electrodes (i.e., heights). For a given electrode, the initial steep increase indicates that the foam formed by air bubbling in the protein solution reached the height of the electrode. The bottom electrode (e07) detects the foam first, the top electrode (e03) detects the foam last. When bubbling is stopped, the liquid fraction reaches a maximum. The higher the electrode, the lower the maximum liquid fraction: this is due to liquid drainage occurring already during the foam formation and upward progression. In the case of Fig. 4a, the maximum liquid fractions range between 0.13 and 0.23.

After bubbling was stopped, typically after less than 1 min, the liquid fraction decreases, reflecting foam destabilisation. If drainage is the main destabilisation process operating, the liquid fraction in foam decreases as a power law of time (Koehler et al., 2000; Saint-Jalmes and Langevin, 2002), illustrated by a linear decrease in log-log representation, and the time exponent reflects the drainage rate. However, after a variable period of time, depending on the electrode and sample, a deviation of this power law regime occurs. In Fig. 4b, for bottom electrodes (e05, e06 and e07), curves have a pronounced rounded shape, followed by a faster liquid fraction decrease. On Fig. 4a, bumps just before 1000 s are visible, corresponding to abrupt water flows from above in the column. So, the drainage is probably coupled with film rupturing (locally popped bubbles and/or disproportionation). Moreover, collective coalescence events, marked by an important decrease of liquid fraction for a very short time, are visible at quite high liquid fraction (1 %) as compared to what is usually found for low molecular weight (LMW) surfactants (Carrier and Colin, 2003). However, electrodes at the top, such as e03, seem more suitable for drainage rate measurements with weak disruption by other instability mechanisms. Finally, this method displays foam variability along the height of the column and between samples.

In the general case, the dual output of PCA consists of i) principal components, which are loadings of the initial variables in the principal components and depict the main dimensions of variability among observations, and ii) scores, which are the coordinates of observations on principal components, used to draw similarity maps where observations are projected. Fig. 5, Fig. 6 and Fig. 7 show the results of PCA on the first two principal components PC1 and PC2. The cumulated proportion of variance accounted for by PC1 and PC2 is 74.5 % (53.0 % and 21.5 %, respectively). PC3 was not considered because it accounted for less than 10 % of total variance. Fig. 5 and Fig. 6 show projections of

observations on the map defined by PC1 and PC2, for all the non dry-heated samples (Fig. 5) and only the dry-heated samples (Fig. 6).

To illustrate the respective meanings of PC1 and PC2 as regards foam profiles, we reconstituted imaginary foams located arbitrarily at coordinates $(\pm 2 \times \sigma_1, 0)$ and $(0, \pm 2 \times \sigma_2)$, where σ_1 and σ_2 are the standard deviations of the sample scores on PC1 and PC2, respectively. In other words, 95% of the samples are between the imaginary samples A and B (for PC1) or C and D (for PC2), assuming a normal distribution. Comparing the corresponding reconstituted, imaginary foam profiles allow to sensibly interpret location on the factorial maps, i.e. scores on PC1 and PC2 in term of foam stability.

Reconstituted imaginary foams A and B in Fig. 7a correspond to samples with low and high scores, respectively, on PC1 (Fig. 5 and Fig. 6). Whatever the electrode (Fig. 7a), over the whole kinetics, the liquid fraction of sample B, decreases slower than the liquid fraction of sample A. Thus, whatever the electrode (Fig. 7a), sample B is more stable than sample A. In addition, the maximum liquid fraction, right after the end of bubbling, tends to be higher for B than for A: for example, at electrode e07, $\varphi_{\max B}=0.23$ while $\varphi_{\max A}=0.20$. In other words, higher scores on PC1 are associated with higher stability and higher maximum foam density.

Reconstituted imaginary foams C and D in Fig. 7b correspond to foams with low and high scores on PC2, respectively (Fig. 5 and Fig. 6). Stability profiles along the foam height are not uniform since they depend on the electrode (Fig. 7b). Sample D has a higher stability at the top of the foam column (Fig. 7b). Indeed, at e03 and e04, the decrease in liquid fraction is slower for sample D than for sample C. The corresponding exponents at electrode e03 are $\alpha_D=0.80$ for D and $\alpha_C=1.10$ for C. However at the bottom of the foam column (e05, e06, e07), kinetics are less linear than at the top (e03, e04), and differences in stability between C and D are less obvious. Concerning the foam formation, the foam is detected earlier for sample D by a given electrode ($t_D=61$ s and $t_C=71$ s at e03) (Fig. 7b). However, this was attributed to an experimental bias and will not be discussed in the following sections.

Finally, samples with a high score on PC1 (i.e. located on the right side of the factorial map) have a high foam stability and density. Samples with a high score on PC2 (i.e. located on the upper part of the factorial map) have a high foam stability at the top of the foam.

Fig. 5 shows the scores on PC1 and PC2 of foams from control samples (1), (2) and (3) and of foams from a_w -conditioned samples at different pH (i.e., prior to dry-heating). Control samples are grouped on the high-PC1-score side of the map and around the average zero score on PC2. In contrast, a_w -conditioned samples are spread over the map, showing that the incubation for two weeks at room temperature for a_w -conditioning markedly affected the foam behaviour, whatever the pH. However, Fig. 5 does not show any clear preferential location of foams on the PC2 versus PC1 map depending on a_w (a) or pH (b).

Fig. 6 shows that dry-heating of whey proteins impacts their foaming behaviour with a complex dependence on dry-heating parameters such as pH prior dehydration for example (Fig. 6b). In more details, dry-heating at pH 5.0, whatever the time, results in low scores on PC1 (Fig. 6b), suggesting low foam stability of these samples. On the other hand, dry-heating for 125 h, whatever the pH prior to dehydration, increases score on PC2 (Fig. 6a), suggesting rather high foam stability at the top of the foam. Those results suggest complex interactions between dry-heating parameters. They also show that the effect of powder pre-conditioning (Fig. 5) is in the same order of magnitude as the effect of subsequent dry-heating (Fig. 6). In order to obtain quantitative estimations of the effects of dry-

heating parameters and their interactions on foam stability, analysis of variance (ANOVA) was performed.

3.2 Dry-heating parameters effects on foam stability

Table 1 presents the significant main effects and their second order interactions, on the coordinates of the samples on PC1 and PC2. The ANOVA estimates and standard errors are given in supplementary materials (Tables A and B).

Table 1 ANOVA *p*-values of the different variables and their significant interactions for PC1 and PC2. For a *p*-value > 0.05 variables and/or interactions were considered as not significant (NS) and were eliminated.

	pH	a_w	time	lactose	pH: a_w	pH:time	a_w :time	pH:lactose	a_w :lactose	time:lactose
PC1	0,0090	0,0022	0,0001	0,0157	NS	0,0001	NS	0,0032	0,0080	NS
PC2	0,0901	0,0055	<10 ⁻⁴	NS	<10 ⁻⁴	<10 ⁻⁴	0,0001	NS	NS	NS

Taking into account all variables and interactions, the R^2 of the models for PC1 and PC2 are 45.42 % and 60.85 %, respectively. These quite medium R^2 scores may be due to the significance of higher order interactions that could not be estimated, due to the use of a fractional experimental design. For the same reason, some interaction estimates on PC1 (pH 3.5:1 h, pH 5.0:1 h, pH 5:25 h) and PC2 (pH 3.5:1 h, pH 5.0:1 h, pH 5.0:25 h and pH 5.0:5 h) could not be calculated (supplementary data). Thus, the corresponding experimental conditions, shown as greyed cells in Fig. 8 and Fig. 9, are not discussed.

Fig. 8 shows the values predicted by the model for scores on PC1 (i.e. foam stability) as a function of pH, dry-heating time and lactose content for samples dry-heated at an a_w of 0.52. This a_w was chosen for data representation because it emphasised the effects of dry-heating. In this case, the optimal foam stability corresponds to no or short dry-heating (0 h or 1 h), whatever the lactose content. However, since the colours are overall lighter for reduced lactose content (Fig. 8a), decreasing the lactose content increases samples scores on PC1, and thus their foam stability. On the opposite, extensive dry-heating (125 h) at pH 5.0 and pH 6.5 decreases the foam stability and the effect strengthens with lactose content (Fig. 8b). In contrast, dry-heating at pH 3.5 preserves or even improves the foam stability for extended dry-heating.

Fig. 9 shows the values predicted by the model for scores on PC2 (i.e. stability at the top of the foam) as a function of a_w and heating time at pH 6.5 (a) and pH and heating time at a_w 0.52 (b). Fig. 9a shows that decreasing a_w of samples dry heated at pH 6.5 (whatever the dry heating time, i.e. even for non-dry heated samples) increases the local stability at the top of the foam. Fig. 9b illustrates that the adjustment of the powder pH to 3.5 (whatever the dry-heating time), or 125 h dry-heating (whatever the pH) also increases the stability at the top of the foam.

The results of ANOVA thus validate the tendencies previously observed on PCA maps (Fig. 5, Fig. 6): they highlight the major role of interactions between pre-conditioning and dry-heating parameters.

Considering the particular results obtained with samples adjusted to pH 3.5 before dry-heating, the experimental design was completed with samples missing at this pH.

3.3 Foam stability at pH 3.5

The data about foam stability from the complete experimental design at pH 3.5 were also analysed independently using PCA. The corresponding results are presented in supplementary data (Fig. A).

The first two principal components at pH 3.5 can be interpreted in the same way as in the case of the fractional design (see 3.1), i.e. PC1 as the global stability of the foam and PC2 as the local stability at the top on the foam. In the following section, only the global foam stability will be considered. The proportion of variance accounted for by PC1 is 49.7 %. As in the case of the overall fractional design, increasing scores on PC1 also corresponds to an increase in the global foam stability. The parameter effects on PC1 scores were also evaluated using ANOVA. Table 2 shows significant parameter main effects (a_w , time) and interactions (a_w :time, time:lactose).

Table 2 ANOVA p-values of main effects and interactions for PC1, for the complete experimental design at pH 3.5. For a p-value higher than 0.05, variables and/or interactions were considered as not significant (NS) and were eliminated. The lactose main effect was kept due to the highly significant time:lactose interaction.

	a_w	time	lactose	a_w :time	a_w :lactose	time:lactose
PC1	0,0021	0,0020	0,6985	0,0008	NS	$<10^{-4}$

The model R^2 is 64.03 %. Fig. 10 illustrates the model predictions for PC1 scores (the estimated effects are provided in supplementary data, Table C).

For short dry-heating (0 and 1 h), lactose enhances foam stability. However, the highest foam stability is obtained after 125 h of dry heating, whatever the lactose content. However, the increase in foam stability is not monotonous, since dry-heating for 5 h with high lactose content strongly decreases the foam stability.

The focus on data at pH 3.5 thus shows that in these conditions, extended dry-heating significantly increases the global foam stability.

4. Discussion

4.1 Principal component analysis of liquid fractions time- and height-profiles allows a detailed comparison of foam stabilities

Monitoring the variation of the liquid fraction ϕ by electrical conductivity measurements is reported in the literature for drainage rates (Koehler et al., 2000; Carey and Stubenrauch, 2013; Daugelaite et al., 2016) and coalescence events measurements (Carrier and Colin, 2003). However, it has been mainly applied to low-molecular-weight (LMW) surfactants foams, which are simpler systems than protein foams. The drainage exponents α inform about both flows at the bubble interface and within the Plateau borders. In our experiments, drainage exponents for whey protein are of the order of $\alpha \approx 0.80$ -1.10 which correspond to immobile interfaces, with slow drainage (Koehler et al., 2000; Saint-Jalmes and Langevin, 2002). Conversely, LMW surfactants usually provide mobile interface and an exponent of $\alpha \approx 2$ (Koehler et al., 2000; Saint-Jalmes and Langevin, 2002). Recently, Daugelaite et al. (2016) had the same approach for egg-white protein foams. They also obtained low drainage exponents ($\alpha \approx 0.5$ -1).

In contrast with forced drainage experiments, used in some of the above-mentioned works, drainage experiments performed in our study are called “free drainage” because the initial liquid fraction gradient is not counterbalanced by re-wetting from the top (Koehler et al., 2000). Consequently, we showed that the liquid fraction time-profiles of whey protein foams are not uniform along the height of the foam column. Indeed, the foam starts draining as soon as it is formed. In addition, as evidenced

by non-linear time-profiles (in log-log plots), drainage and coalescence occur simultaneously. Thus, the water flow at any layer of the foam integrates what happens above, and that is why the top electrode pair (e03) generally shows a more linear time-profile than the other ones, which is suitable for a drainage study. Since the time-profiles are not uniform along the height of the foam, it is necessary to study simultaneously the height- and time-profiles of foam liquid fractions. The large amount of resulting data motivates the use of multivariate statistical analysis, such as principal component analysis (PCA).

Interestingly, this approach clearly shows that foam stability has a ‘global’ dimension (which does not depend on the height), and a ‘local’ dimension (which distinguishes the time-profiles of top and bottom electrodes). The former is illustrated by our PC1, the latter by our PC2. However the technique we used also give information about foam density and foam formation, which also contribute to PC1 and PC2, making the analysis slightly difficult.

In the present work, a focus was made on the stability of foams against drainage. Nevertheless collective coalescence events were also observed (Fig. 4). Bubble coalescence represents a process of thin liquid film rupture between two neighboring bubbles. Factors such as disjoining pressure, film lamella thickness or surface elasticity control the foam stability against coalescence (Narsimhan and Xiang, 2017). In our study, the ionic strength of protein solutions was low. In such conditions, β -lg shows higher film thickness and disjoining pressure, and lower surface elasticity than at high ionic strength (Gochev et al., 2014). This is probably due to unscreened electrostatic repulsions between protein molecules inside the interfacial layer, as well as between the two interfacial layers of the liquid lamella. The occurrence of collective coalescence could then be explained by the low surface elasticity of adsorbed protein films.

4.2 a_w pre-conditioning at room temperature significantly impacts foam stability.

To control a_w , it was necessary to pre-condition powders at 20 °C for two weeks in the presence of saturated salt solutions. Surprisingly, our results clearly show that this pre-conditioning significantly changed foaming properties, even in the absence of any heat-treatment (Fig. 8, Fig. 9 and Fig. 10).

It has been shown that dairy powders stored under solid state may indeed undergo physico-chemical changes with time, like Maillard reaction and oxidation (Rao et al., 2016). These changes occur close to or above the powder glass transition temperatures (T_g), or after long storage time as compared to the time scale of molecular diffusion (Rao et al., 2016). The monitoring of a_w is crucial since the glass transition temperature T_g of dehydrated milk products decrease from 60°C to 0°C with the increase of a_w from 0.1 to 0.5. The temperature T_g also depends on sugar content (Thomas et al., 2004). In our study, powder lactose content was involved in foam stability changes (Fig. 8 and Fig. 10). Thus, since the presence of lactose during the powder storage is known to lead to lactosylation (i.e. condensation between sugar and protein amino groups (glycation)), this chemical modification may be proposed to impact their foaming properties. According to Thomas et al. (2004), nearly all the β -lg is lactosylated after one week of storage (a_w 0.45 at 37°C). Even at low temperatures in milk powders, lactosylation occurs especially when storage temperature exceeds 20°C.

However, our statistical analysis revealed that lactose acts differently on foaming properties depending on pH. Indeed, lactose improved foam stability at pH 3.5 but decreased it at pH 6.5 and a_w 0.52. Consistently, pH effects on protein powder glycation have already been observed (Povey et al., 2009; Thomsen et al., 2012).

Moreover, other modifications could be considered during storage of WPI such as copolymer formation of α -La and β -lg due to free sulfhydryl group oxidation and exchange between proteins (Alting et al., 2003; Thomas et al., 2004).

Finally, complex interactions between the pH, a_w and lactose could explain the changes of foaming properties for samples that have not been dry-heated, even at short storage time at 20 °C. Considering the results of this study, to keep good foaming properties, lactose content of WPI powders should be reduced or, WPI powder pH and/or a_w should be decreased. Otherwise, the manufacturers could also store dairy powders at 4°C according to Norwood et al. (2016) in order to preserve protein functional properties. Indeed, the control of whey protein aggregation is perturbed by WPI powder ageing. Up to date, dairy powder ageing remains an industrial concern, responsible for uncontrolled technological variability (Haque and Bhandari, 2015; Nasser et al., 2017).

4.3 Dry-heating parameters interactions impacts foam properties.

Our study shows that extensive dry-heating (125 h) leads to a wide range of global foam stability, depending on the powder properties (Fig. 6a). In statistical terms, this is reflected by complex interactions between parameters, especially pH:time.

That complexity in parameters effects on foam stability suggest a parallel with the complexity of pH and heating time effects on structural and biochemical changes in WPI: mechanisms and kinetics of aggregation, lactosylation, extent of Maillard reactions (Gulzar et al., 2012; Guyomarc'h et al., 2015). Such structural changes and aggregation conditions have been shown to impact foam stability (Rullier et al., 2008; Fameau and Salonen, 2014).

Fig. 8 shows that extensive dry-heating (125 h) at pH 5.0 and pH 6.5 decreased foam stability, and this effect strengthens with increasing lactose content. On the contrary, dry-heating for 125 h at pH 3.5 with lactose improved foam stability (Fig. 10). This observation suggests the existence of a significant statistical three-way pH:time:lactose interaction, which could not be evaluated due to the choice of a fractional experimental design. Indeed, Guyomarc'h et al. (2015) showed that Maillard reaction products are involved in the formation of aggregates differently depending on the WPI pH prior dry-heating. Acidic condition have been shown to limit Maillard reaction, both in powders (Guyomarc'h et al., 2015) and solution (Wang et al., 2013).

High a_w values may favour chemical reactions, promoting both lactosylation and complex Maillard products. It seems that parameters that are favourable to Maillard reaction (lactose, high pH and a_w) decrease foam stability. However, it is worth noting that when this reaction is limited (at pH 3.5), dry-heating increases foam stability even with high lactose content and high a_w .

Our study also shows that extensive treatment (125 h) improves the local stability against drainage at the top of the foam, as reflected by high scores on PC2. A possible explanation is that aggregates probably act as obstacles to liquid flow during the confinement inside the foam (Fameau and Salonen, 2014).

Still, in our experiments at pH 3.5, even in conditions unfavourable to the formation of aggregates (no or short dry-heating), the local stability was increased. This suggests that interfacial rheology is involved in those observations, as corroborated by the changes in the drainage time exponent, related to interfacial mobility (Koehler et al., 2000; Saint-Jalmes and Langevin, 2002). Thus, a possible explanation is that the drainage is limited at pH 3.5 because of small structural modification with a large impact on foaming properties.

Finally, bulk properties, through the presence of aggregates restricting the flow, as well as interfacial properties, through the interfacial rheology, could both explain the extent in the observed variations of the drainage exponent (α).

Thus, WPI dry-heated at pH 3.5 could be used as a foam stabiliser for ice-cream, coffee whitener or meringues applications (Suthar et al., 2017). Nevertheless, conditions promoting extensive Maillard reaction may also reduce foaming properties, thus justifying a de-sugaring process step, as commonly performed in egg white industrial processing (Campbell et al., 2003).

5. Conclusions

In the present work, we examined the effect of powder dry-heating time, under controlled physicochemical conditions (a_w , pH prior to dehydration and lactose content), on whey protein foam stability. Principal component analysis of the liquid fraction time- and height-profiles of about 150 whey protein foams allows a detailed comparison of foam stabilities. Interestingly, this sensitive approach clearly shows that foam stability has a ‘global’ dimension (which do not depend of height), and a ‘local’ dimension (which distinguishes the time-profiles of top and bottom electrodes). Interactions between pH prior to dehydration, powder a_w , lactose content and dry-heating time at 70°C caused complex effects of dry-heating on foam stability. Extensive dry-heating at pH 5.0 and pH 6.5 lower the global foam stability and the effect strengthens with lactose content. Nevertheless, dry-heating at pH 3.5 preserves the foam stability, including for extended dry-heating. We propose that pH 3.5 has a protective effect against Maillard reactions, which are detrimental to foam stability, as compared to pH 5.0 and 6.5. Surprisingly, storage of powders for two weeks at room temperature prominently impacted foaming properties. These results suggest that even in the absence of a thermal treatment of the powder, protein structural changes and modifications of interfacial properties may occur. Our findings point at the need for a thorough characterisation of protein structural and biochemical changes in WPI during storage and upon dry-heating. Such a characterisation is in progress. Relating foaming properties to protein features remains a crucial challenge.

Acknowledgements

We are grateful to the Regional councils of Brittany (grant N° 13008651) and Pays de la Loire (grant N°2014-07081) for their financial support as well as INRA for its scientific coordination (J. Leonil) through the interregional project PROFIL, managed by the BBA industrial association.

References

- Abdi, H., Williams, L.J., 2010. Principal component analysis. Wiley Interdiscip. Rev. Comput. Stat. 2, 433–459. <https://doi.org/10.1002/wics.101>
- Alting, A.C., Hamer, R.J., de Kruif, C.G., Paques, M., Visschers, R.W., 2003. Number of thiol groups rather than the size of the aggregates determines the hardness of cold set whey protein gels. Food Hydrocoll. 17, 469–479. [https://doi.org/10.1016/S0268-005X\(03\)00023-7](https://doi.org/10.1016/S0268-005X(03)00023-7)
- Anema, S.G., 2014. Chapter 9 - The Whey Proteins in Milk: Thermal Denaturation, Physical Interactions, and Effects on the Functional Properties of Milk, in: Singh, H., Boland, M., Thompson, A. (Eds.), Milk Proteins (Second Edition), Food Science and Technology.

- Academic Press, San Diego, pp. 269–318. <https://doi.org/10.1016/B978-0-12-405171-3.00009-X>
- Arena, S., Renzone, G., D'Ambrosio, C., Salzano, A.M., Scaloni, A., 2017. Dairy products and the Maillard reaction: A promising future for extensive food characterization by integrated proteomics studies. *Food Chem.* 219, 477–489. <https://doi.org/10.1016/j.foodchem.2016.09.165>
- Boreddy, S.R., Thippareddi, H., Froning, G., Subbiah, J., 2016. Novel Radiofrequency-Assisted Thermal Processing Improves the Gelling Properties of Standard Egg White Powder. *J. Food Sci.* 81, E665–671. <https://doi.org/10.1111/1750-3841.13239>
- Campbell, L., Raikos, V., Euston, S.R., 2003. Modification of functional properties of egg white proteins. *Food Nahr.* 47, 369–376. <https://doi.org/10.1002/food.200390084>
- Cantat, I., Cohen-Addad, S., Elias, F., Graner, F., Höhler, R., Pitois, O., Rouyer, F., Saint-Jalmes, A., 2013. *Foams: Structure and Dynamics*. OUP Oxford.
- Carey, E., Stubenrauch, C., 2013. Free drainage of aqueous foams stabilized by mixtures of a non-ionic (C12DMPO) and an ionic (C12TAB) surfactant. *Colloids Surf. Physicochem. Eng. Asp.* 419, 7–14. <https://doi.org/10.1016/j.colsurfa.2012.11.037>
- Carrier, V., Colin, A., 2003. Coalescence in Draining Foams. *Langmuir* 19, 4535–4538. <https://doi.org/10.1021/la026995b>
- Chevallier, M., Riaublanc, A., Lopez, C., Hamon, P., Rousseau, F., Thevenot, J., Croguennec, T., 2018. Increasing the heat stability of whey protein-rich emulsions by combining the functional role of WPM and caseins. *Food Hydrocoll.* 76, 164–172. <https://doi.org/10.1016/j.foodhyd.2016.12.014>
- Corzo-Martínez, M., Carrera Sánchez, C., Moreno, F.J., Rodríguez Patino, J.M., Villamiel, M., 2012. Interfacial and foaming properties of bovine β -lactoglobulin: Galactose Maillard conjugates. *Food Hydrocoll.* 27, 438–447. <https://doi.org/10.1016/j.foodhyd.2011.11.003>
- Daugelaite, D., Guillermic, R.-M., Scanlon, M.G., Page, J.H., 2016. Quantifying liquid drainage in egg-white sucrose foams by resistivity measurements. *Colloids Surf. Physicochem. Eng. Asp.* 489, 241–248. <https://doi.org/10.1016/j.colsurfa.2015.10.053>
- Desfougères, Y., Saint-Jalmes, A., Salonen, A., Vié, V., Beaufils, S., Pezenec, S., Desbat, B., Lechevalier, V., Nau, F., 2011. Strong Improvement of Interfacial Properties Can Result from Slight Structural Modifications of Proteins: The Case of Native and Dry-Heated Lysozyme. *Langmuir* 27, 14947–14957. <https://doi.org/10.1021/la203485y>
- Fameau, A.-L., Salonen, A., 2014. Effect of particles and aggregated structures on the foam stability and aging. *Comptes Rendus Phys.* 15, 748–760. <https://doi.org/10.1016/j.crhy.2014.09.009>
- Feitosa, K., Marze, S., Saint-Jalmes, A., Durian, D.J., 2005. Electrical conductivity of dispersions: from dry foams to dilute suspensions. *J. Phys. Condens. Matter* 17, 6301–6305. <https://doi.org/10.1088/0953-8984/17/41/001>
- Gochev, G., Retzlaff, I., Exerowa, D., Miller, R., 2014. Electrostatic stabilization of foam films from β -lactoglobulin solutions. *Colloids Surf. Physicochem. Eng. Asp.* 460, 272–279. <https://doi.org/10.1016/j.colsurfa.2013.12.037>
- Gulzar, M., Bouhallab, S., Jeantet, R., Schuck, P., Croguennec, T., 2011. Influence of pH on the dry heat-induced denaturation/aggregation of whey proteins. *Food Chem.* 129, 110–116. <https://doi.org/10.1016/j.foodchem.2011.04.037>
- Gulzar, M., Lechevalier, V., Bouhallab, S., Croguennec, T., 2012. The physicochemical parameters during dry heating strongly influence the gelling properties of whey proteins. *J. Food Eng.* 112, 296–303. <https://doi.org/10.1016/j.jfoodeng.2012.05.006>
- Guyomarc'h, F., Famelart, M.-H., Henry, G., Gulzar, M., Leonil, J., Hamon, P., Bouhallab, S., Croguennec, T., 2015. Current ways to modify the structure of whey proteins for specific functionalities-a review. *Dairy Sci. Technol.* 95, 795–814. <https://doi.org/10.1007/s13594-014-0190-5>
- Haque, E., Bhandari, B.R., 2015. Effects of Protein Conformational Modifications, Enthalpy Relaxation, and Interaction with Water on the Solubility of Milk Protein Concentrate Powder, in: *Water Stress in Biological, Chemical, Pharmaceutical and Food Systems*, Food Engineering Series. Springer, New York, NY, pp. 437–450. https://doi.org/10.1007/978-1-4939-2578-0_38

- 525 Koehler, S.A., Hilgenfeldt, S., Stone, H.A., 2000. A Generalized View of Foam Drainage: Experiment
526 and Theory. *Langmuir* 16, 6327–6341. <https://doi.org/10.1021/la9913147>
- 527 Lazidis, A., Hancocks, R.D., Spyropoulos, F., Kreuß, M., Berrocal, R., Norton, I.T., 2016. Whey
528 protein fluid gels for the stabilisation of foams. *Food Hydrocoll.* 53, 209–217.
529 <https://doi.org/10.1016/j.foodhyd.2015.02.022>
- 530 Medrano, A., Abirached, C., Panizzolo, L., Moyna, P., Añón, M.C., 2009. The effect of glycation on
531 foam and structural properties of β -lactoglobulin. *Food Chem.* 113, 127–133.
532 <https://doi.org/10.1016/j.foodchem.2008.07.036>
- 533 Narsimhan, G., Xiang, N., 2017. Role of Proteins on Formation, Drainage, and Stability of Liquid
534 Food Foams. *Annu. Rev. Food Sci. Technol.* <https://doi.org/10.1146/annurev-food-030216-030009>
- 535 Nasser, S., Moreau, A., Jeantet, R., Hédoux, A., Delaplace, G., 2017. Influence of storage conditions
536 on the functional properties of micellar casein powder. *Food Bioprod. Process.* 106, 181–192.
537 <https://doi.org/10.1016/j.fbp.2017.09.004>
- 538 Nicorescu, I., Vial, C., Talansier, E., Lechevalier, V., Loisel, C., Della Valle, D., Riaublanc, A.,
539 Djelveh, G., Legrand, J., 2011. Comparative effect of thermal treatment on the
540 physicochemical properties of whey and egg white protein foams. *Food Hydrocoll.* 25, 797–
541 808. <https://doi.org/10.1016/j.foodhyd.2010.09.020>
- 542 Norwood, E.-A., Chevallier, M., Le Floch-Fouéré, C., Schuck, P., Jeantet, R., Croguennec, T., 2016.
543 Heat-Induced Aggregation Properties of Whey Proteins as Affected by Storage Conditions of
544 Whey Protein Isolate Powders. *Food Bioprocess Technol.* 9, 993–1001.
545 <https://doi.org/10.1007/s11947-016-1686-1>
- 546 Norwood, E. -A., Le Floch-Fouéré, C., Briard-Bion, V., Schuck, P., Croguennec, T., Jeantet, R., 2016.
547 Structural markers of the evolution of whey protein isolate powder during aging and effects
548 on foaming properties. *J. Dairy Sci.* 99, 5265–5272. <https://doi.org/10.3168/jds.2015-10788>
- 549 Ortega-Requena, S., Rebouillat, S., 2015. Retracted Article: Bigger data open innovation: potential
550 applications of value-added products from milk and sustainable valorization of by-products
551 from the dairy industry. *Green Chem.* 17, 5100–5113. <https://doi.org/10.1039/C5GC01428J>
- 552 Povey, J.F., Perez-Moral, N., Noel, T.R., Parker, R., Howard, M.J., Smales, C.M., 2009. Investigating
553 variables and mechanisms that influence protein integrity in low water content amorphous
554 carbohydrate matrices. *Biotechnol. Prog.* 25, 1217–1227. <https://doi.org/10.1002/btpr.207>
- 555 R Core Team, 2017. R: A language and environment for statistical computing [WWW Document].
556 URL <https://www.r-project.org/> (accessed 5.16.18).
- 557 Radwan, I.H., Kobayashi, K., Kato, A., 1993. Improvement of the Surface Functional Properties of β -
558 Lactoglobulin and α -Lactalbumin by Heating in a Dry State. *Biosci. Biotechnol. Biochem.* 57,
559 1549–1552. <https://doi.org/10.1271/bbb.57.1549>
- 560 Rao, Q., Kamdar, A.K., Labuza, T.P., 2016. Storage Stability of Food Protein Hydrolysates—A
561 Review. *Crit. Rev. Food Sci. Nutr.* 56, 1169–1192.
562 <https://doi.org/10.1080/10408398.2012.758085>
- 563 Rullier, B., Novales, B., Axelos, M.A.V., 2008. Effect of protein aggregates on foaming properties of
564 β -lactoglobulin. *Colloids Surf. Physicochem. Eng. Asp.* 330, 96–102.
565 <https://doi.org/10.1016/j.colsurfa.2008.07.040>
- 566 Saint-Jalmes, A., 2006. Physical chemistry in foam drainage and coarsening. *Soft Matter* 2, 836.
567 <https://doi.org/10.1039/b606780h>
- 568 Saint-Jalmes, A., Langevin, D., 2002. Time evolution of aqueous foams: drainage and coarsening. *J.*
569 *Phys. Condens. Matter* 14, 9397–9412. <https://doi.org/10.1088/0953-8984/14/40/325>
- 570 Schmitt, C., Bovay, C., Rouvet, M., 2014. Bulk self-aggregation drives foam stabilization properties
571 of whey protein microgels. *Food Hydrocoll.* 42, 139–148.
572 <https://doi.org/10.1016/j.foodhyd.2014.03.010>
- 573 Schuck, P., Jeantet, R., Dolivet, A., 2012. Analytical Methods for Food and Dairy Powders. John
574 Wiley & Sons.
- 575 Suthar, J., Jana, A., Smitha Balakrishnan, 2017. High Protein Milk Ingredients - A Tool for Value-
576 Addition to Dairy and Food Products. *J. Dairy Vet. Anim. Res.* 6, 1–7.
577 <https://doi.org/10.15406/jdvar.2017.6.00171>
- 578

- 579 Thomas, M.E.C., Scher, J., Desobry-Banon, S., Desobry, S., 2004. Milk Powders Ageing: Effect on
580 Physical and Functional Properties. *Crit. Rev. Food Sci. Nutr.* 44, 297–322.
581 <https://doi.org/10.1080/10408690490464041>
- 582 Thomsen, M.K., Olsen, K., Otte, J., Sjøstrøm, K., Werner, B.B., Skibsted, L.H., 2012. Effect of water
583 activity, temperature and pH on solid state lactosylation of β -lactoglobulin. *Int. Dairy J.* 23,
584 1–8. <https://doi.org/10.1016/j.idairyj.2011.10.008>
- 585 Wang, Q., He, L., Labuza, T.P., Ismail, B., 2013. Structural characterisation of partially glycosylated
586 whey protein as influenced by pH and heat using surface-enhanced Raman spectroscopy.
587 *Food Chem.* 139, 313–319. <https://doi.org/10.1016/j.foodchem.2012.12.050>
- 588 Zhou, P., Labuza, T.P., 2007. Effect of Water Content on Glass Transition and Protein Aggregation of
589 Whey Protein Powders During Short-Term Storage. *Food Biophys.* 2, 108–116.
590 <https://doi.org/10.1007/s11483-007-9037-4>
591

Figure captions

Figure 1. Preparation of samples. (1), (2) and (3) were control samples. Sample (1) underwent only the precipitation at pH 4.6. Besides the precipitation, (2) was freeze-dried at pH 3.5 and (3) at pH 6.5. D samples have a 10 times lower amount of lactose than L samples which keep their native amount in lactose.

Figure 2. Schematic representation of the foam column (height 50 cm and diameter 2 cm) in which 10 pairs of electrodes (e_x) are embedded, facing each other along the height at equal distance.

Figure 3. Picture of whey protein foam by CCD camera.

Figure 4. Typical log-log plots of the liquid fraction of WPI foams as a function of time at different electrodes (e_x). Figure 4a and 4b show two different foams sharing the same parameters (0 h, D, a_w 0.52) except their pH prior to dehydration, pH 5.0 and pH 3.5 respectively. The exponent α or drainage rate is represented by a dashed line at e_{03} as an example.

Figure 5. Factorial maps of scores on PC2 vs PC1 of non dry heated samples (42 samples among the 143 used to performed the PCA) represented according to their a_w (a) or pH (b). Each circle corresponds to one foam, and the filled colour depends on the value of the indicated parameter. The size of the circles figures the individual projection quality on the map: the larger the circle, the better the projection. Control samples without a_w adjustment are represented by numbers surrounded by a black circle, as detailed in section 2.2.1. Samples A, B, C, and D are imaginary samples reconstituted as explained in the text (section 3.1).

Figure 6. Factorial maps of scores on PC2 vs PC1 of dry-heated samples (101 samples among the 143 used to performed the PCA) represented according to their dry-heating time (a) or pH (b). Each circle corresponds to one foam, and the filled colour depends on the value of the indicated parameter. The size of the circles figures the individual projection quality on the map: the larger the circle, the better the projection. Samples A, B, C, and D are imaginary samples reconstituted as explained in the text (section 3.1).

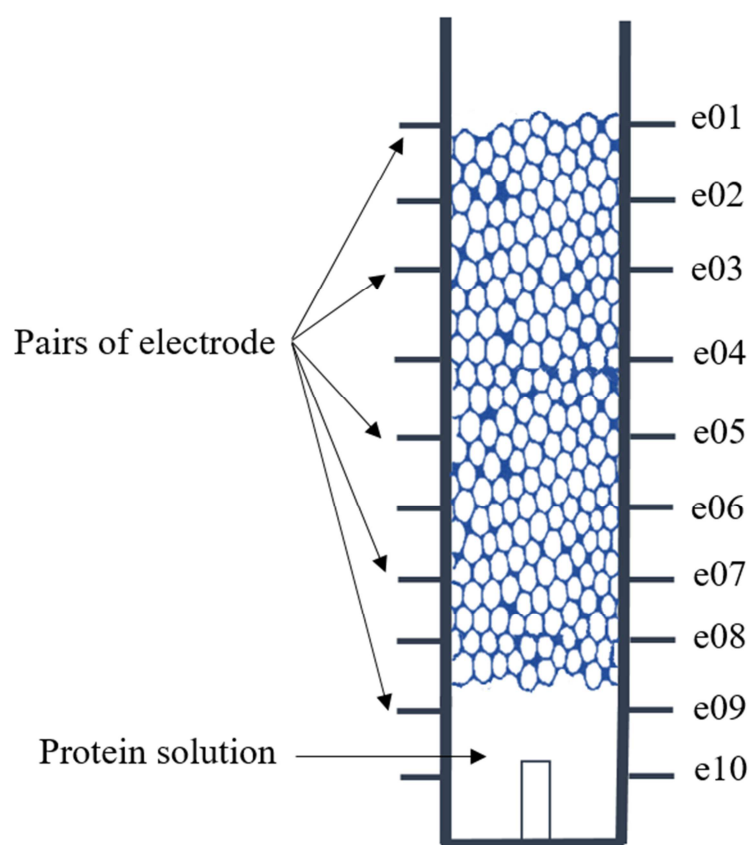
Figure 7. Liquid fraction profiles calculated for imaginary samples A and B on PC1 (a) and C and D on PC2 (b). A and B (C and D, respectively) are located at plus or minus twice the standard deviations from the mean sample score on PC1 (PC2, respectively), as explained in the text (section 3.1).

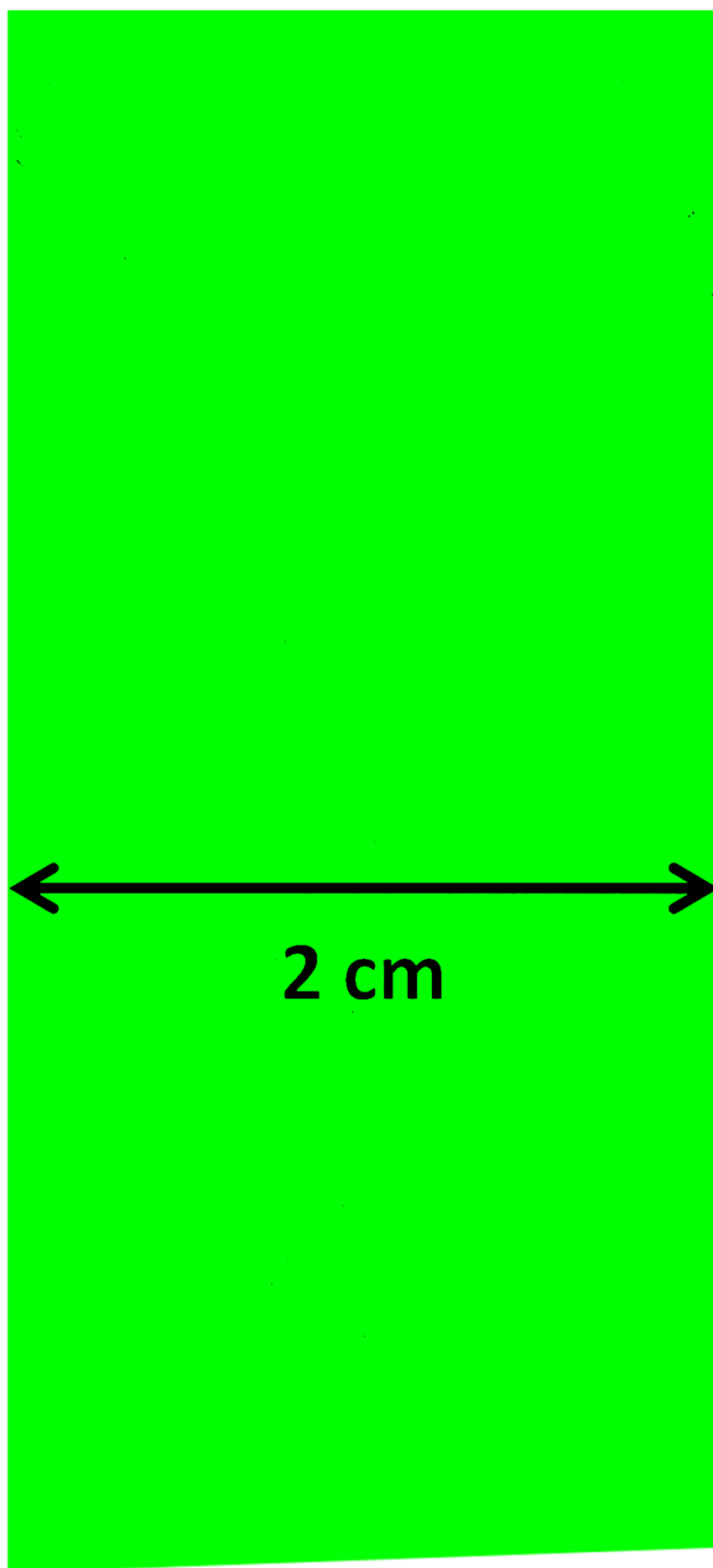
Figure 8. Graphical representations of values predicted by the model for scores on PC1 as a function of pH and heating time at a_w 0.52 with (a) a reduced amount of lactose “D” and (b) the initial amount of lactose “L”. Each cell is coloured according to the predicted score on PC1. The higher the predicted score on PC1 the higher the foam stability. Greyed cells correspond to missing estimations due to the fractional experimental design.

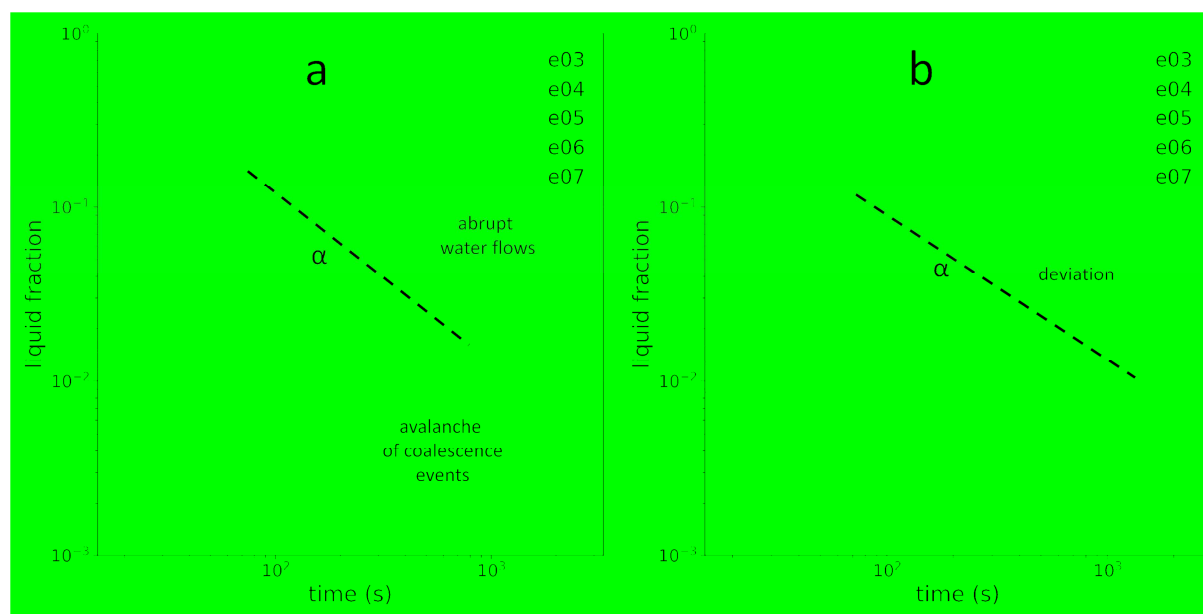
Figure 9. Graphical representations of values predicted by the model for scores on PC2 as a function of a_w and heating time at pH 6.5 (a) and pH and heating time at a_w 0.52 (b). Each cell is coloured according to the predicted score on PC2. The higher the predicted score on PC2

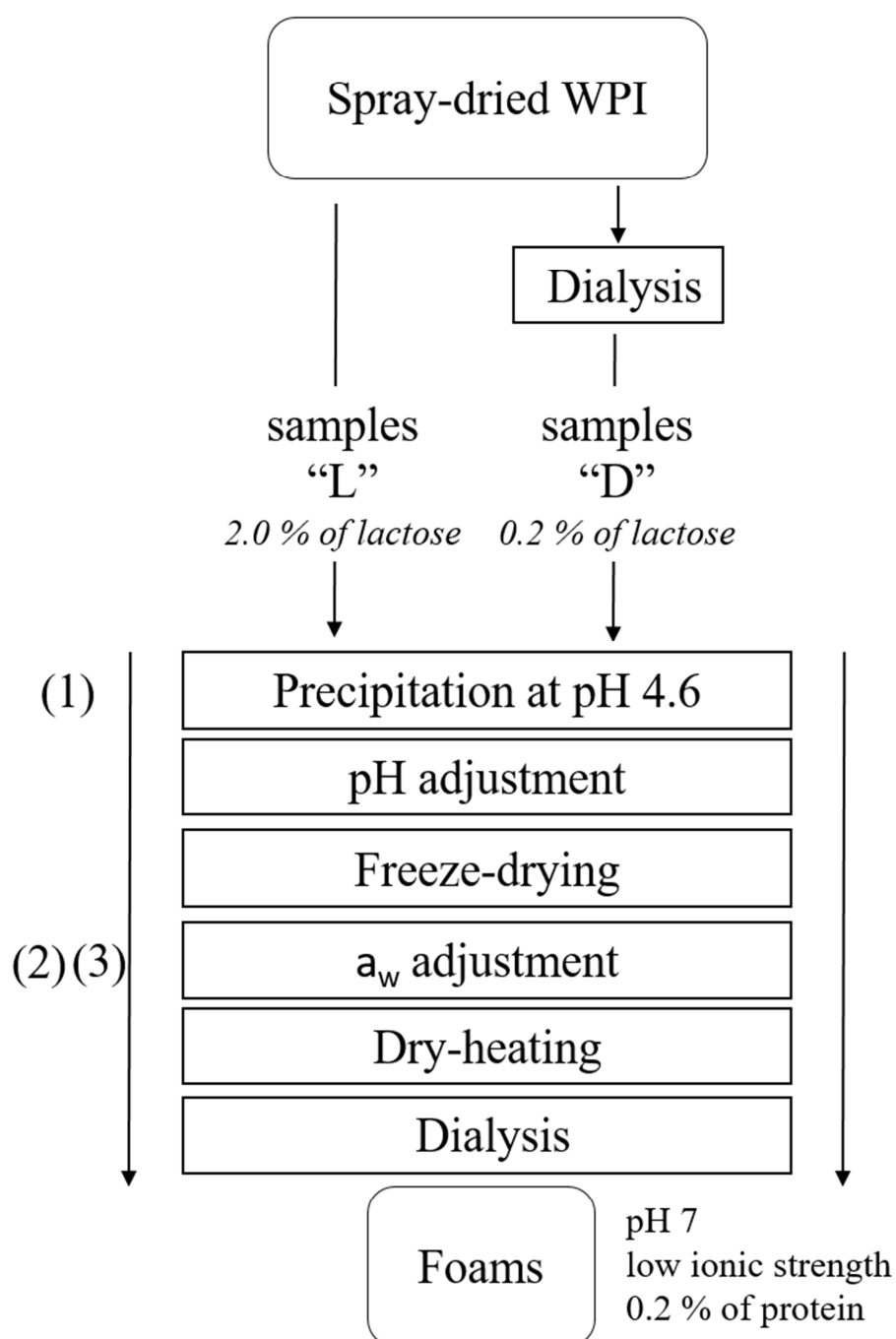
the higher the foam stability at the top of the foam. Greyed cells correspond to missing estimations due to the fractional experimental design.

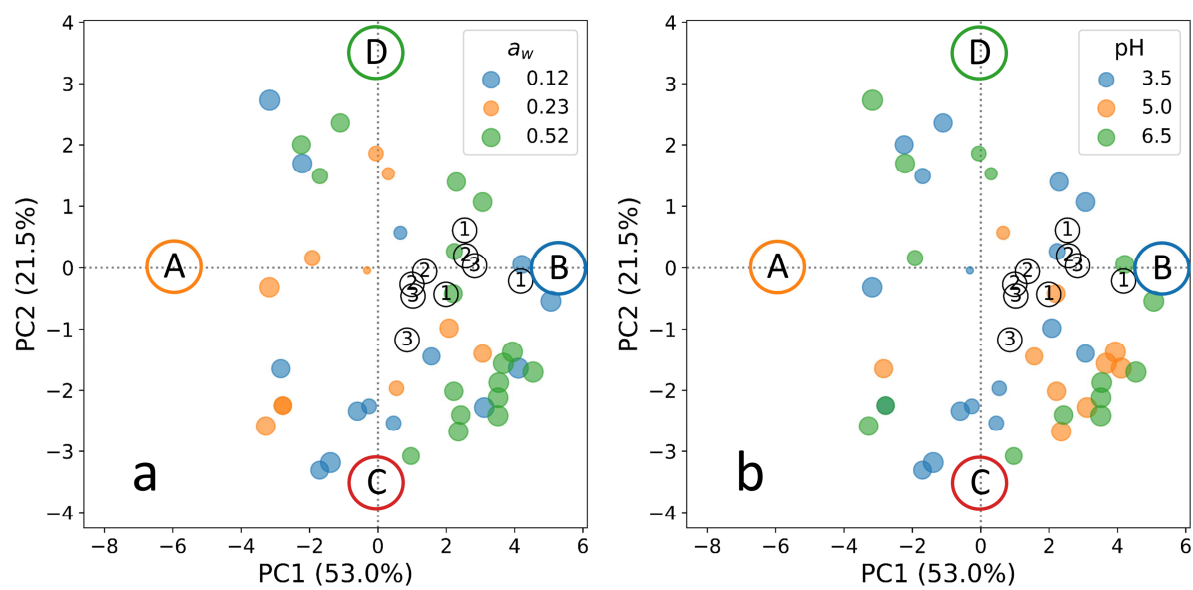
Figure 10. Graphical representation of the model predictions for PC1 of the PCA performed on the complete factorial design at pH 3.5, as a function of lactose content and dry-heating time at a_w 0.52 and pH 3.5. Each cell is coloured according to the predicted score on PC1. The higher the predicted score on PC1 the higher the foam stability.

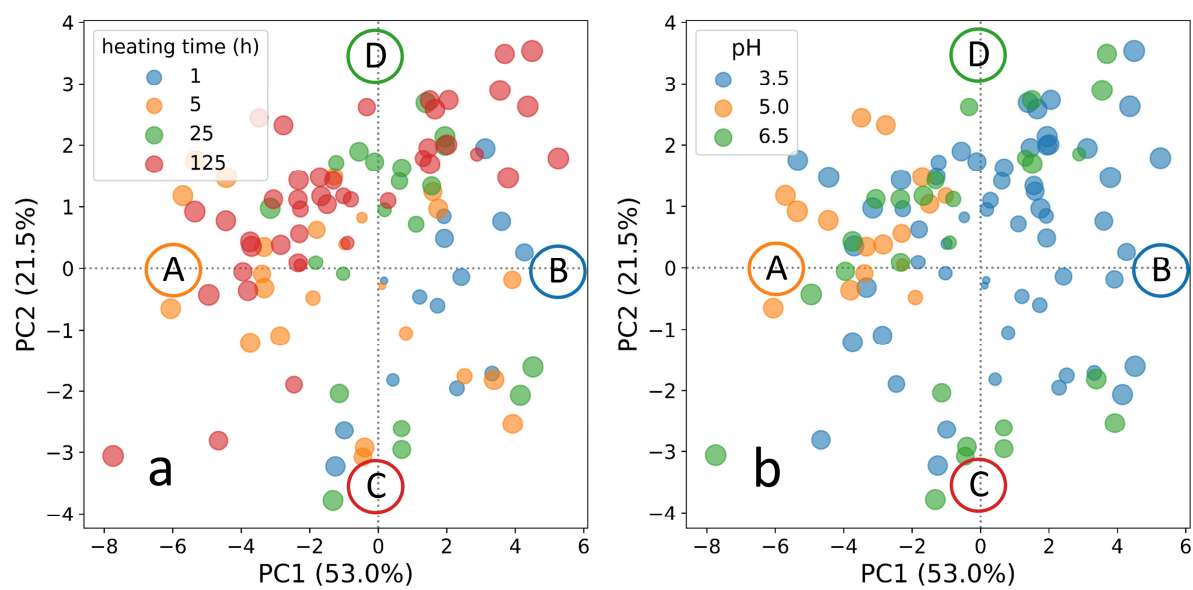


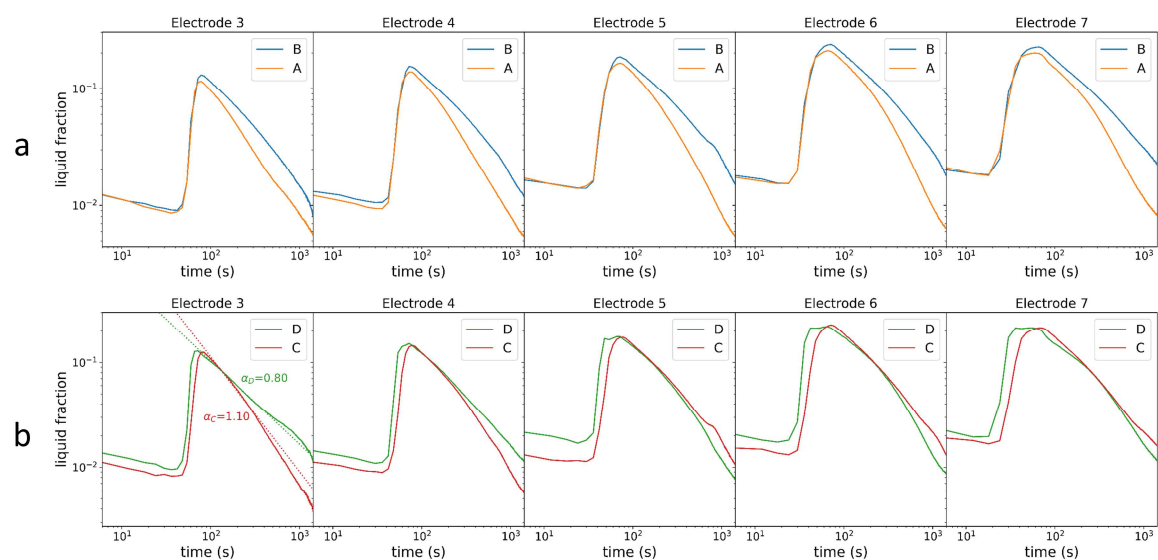


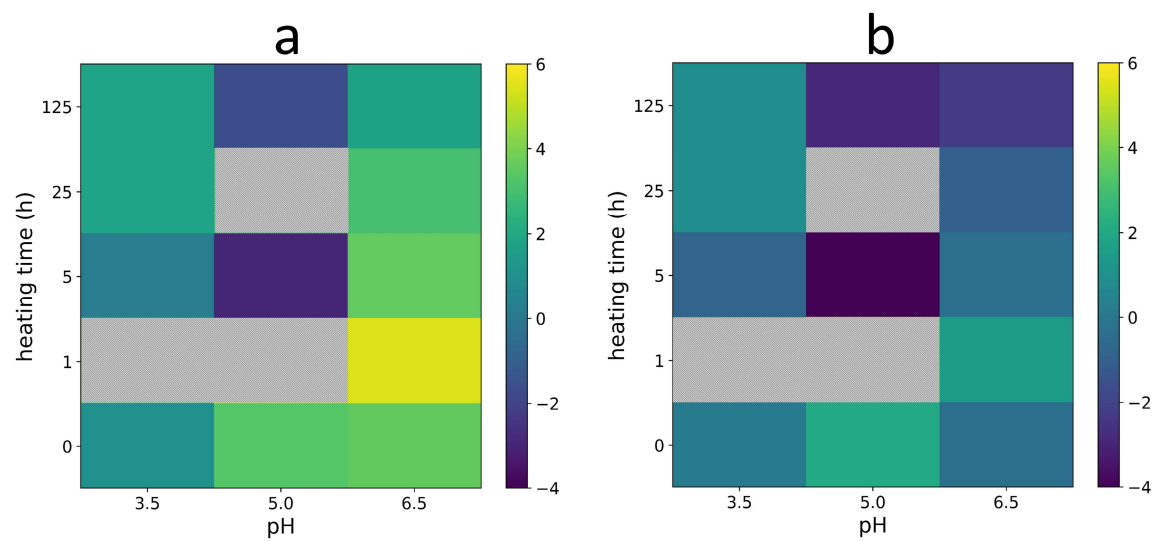


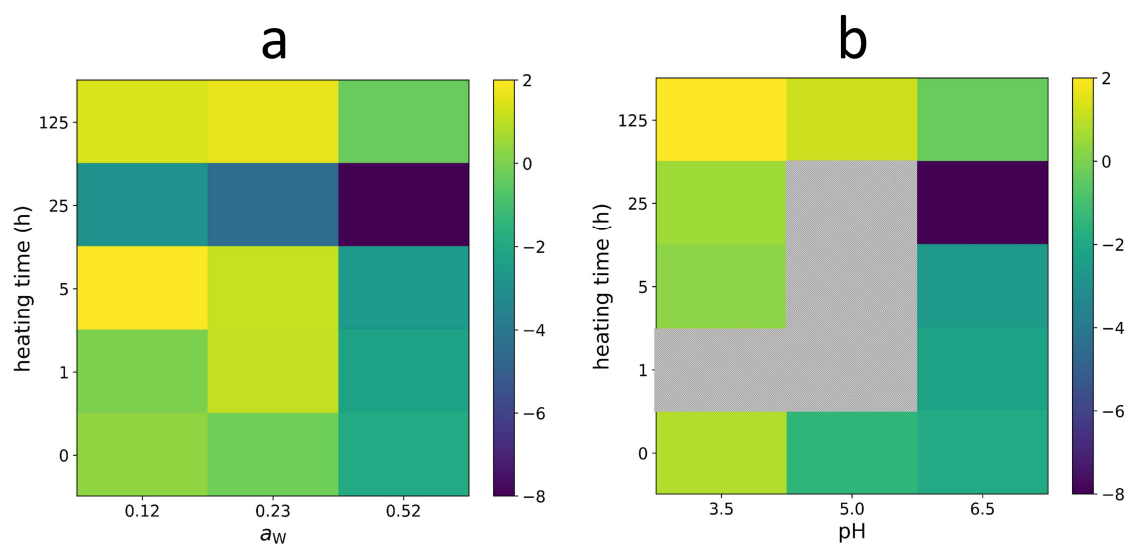


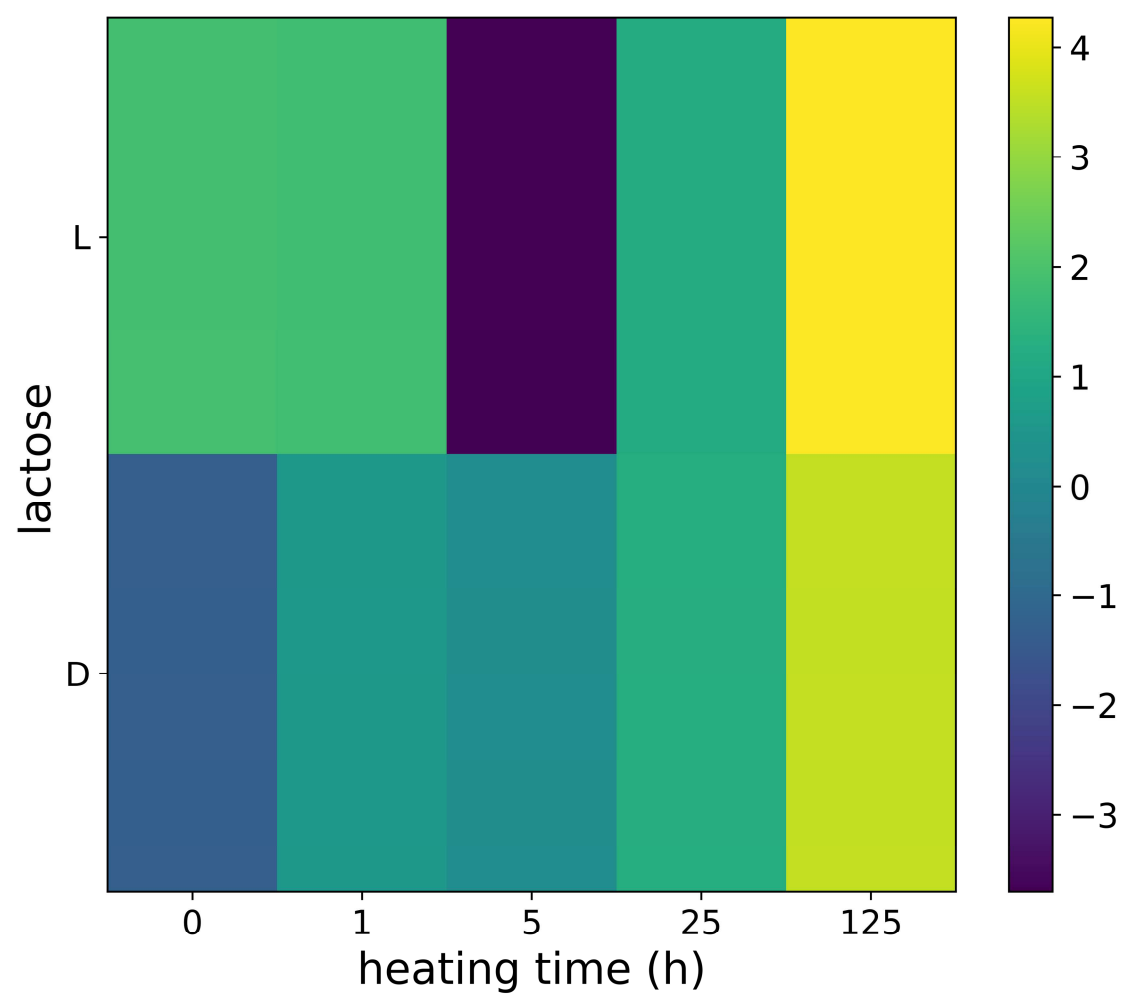












Highlights

- We monitored drainage using time and height liquid fraction profiles
- Multivariate statistics allow comparison of foam stabilities
- Storage of powders prominently impacted foam stability
- Powder dry-heating parameters caused complex effects on foam stability